

Self-similar expansion model of cylindrical flux ropes combined with Alfvén wave current system

Hironori Shimazu

National Institute of Information and Communications Technology, Seika, Kyoto

619-0289, Japan

Email: hironori.shimazu@gmail.com

February 13, 2019

ABSTRACT

Magnetic flux ropes in space are generally connected to some regions electromagnetically. We consider the whole closed current system of the expanding flux ropes including the electric current associated with them. By combining the theories regarding the self-similar expansion of cylindrical flux ropes and the Alfvén wave current system, we examine conditions under which the electric current matches. These matching conditions are satisfied when the time dependence of the current flowing in the closed circuit agrees with that which maintains the expanding flux rope. In consequence, we encountered three possible forms of expansion. The two-step eruption of solar filaments may be interpreted as a transition from one form of expansion to another. If this process works, increasing the diffusion outside of the flux rope is necessary to trigger the transition.

1 Introduction

Magnetic flux ropes are magnetohydrodynamics (MHD) structures, in which the force-free state of the magnetic field is almost maintained by the electric current flowing along the field lines. They are often observed in eruptive prominences and cores of coronal mass ejections (CMEs) in the field of view of space-borne coronagraphs (Gary and Moore, 2004; Patsourakos et al., 2013; Cheng et al., 2014; Joshi et al., 2014). While propagating in interplanetary space, flux ropes expand with distance from the Sun (Burlaga et al., 1981; Marubashi, 1986). Following the launch of CMEs, the magnetic structure measured in space is identified with the flux rope arriving near the Earth (Lepping et al., 1990; Dasso et al., 2007). While some doubts have been raised whether flux ropes exist before eruptions (Panasenco et al., 2014), many alternative configurations transform into flux ropes via reconnection at the start of the eruptive process (DeVore and Antiochos, 2000; Aulanier et al., 2010).

The expansion of the flux rope has often been considered to be self-similar. The technique of converting time derivatives into self-similar expansion parameters in MHD equations was originally applied by Bernstein and Kulsrud (1965) and Kulsrud et al. (1965) to supernova explosions. The self-similar approach simplifies the time-dependent problems and makes them analytically tractable. Low (1982) found a class of spherical self-similar solutions of the expanding solar corona. Kumar and Rust (1996) showed that by assuming the total magnetic helicity is conserved a flux rope evolves self-similarly. Gibson and Low (1998) used the same approach, and presented a theoretical MHD model describing the time-dependent expulsion of a CME.

The models of the expansion of the cylindrical flux ropes can be categorized as either expansions in all directions, called 3D expansions, or those that do not include an axial expansion, i.e., only radial expansion, called 2D expansions (see Figure 1). Osherovich et al. (1993; 1995) analyzed the MHD equations and found a class of self-similar solutions for 2D expansions. They showed that for this class of self-similar solutions cylindrical flux ropes continued to expand only when the polytropic index γ is less than 1.

Models of the 3D self-similar expansions for cylindrical flux ropes were developed by Shimazu and Vandas (2002) and Berdichevsky et al. (2003). Shimazu and Vandas (2002) showed theoretically that flux ropes continue to expand self-similarly in medium of any γ . That is, 3D expansions are more applicable in space. Theoretical models (Chen and Garren, 1993; Chen, 1996) and MHD simulations (Vandas et al., 1995; Wu et al., 1997; Odstrčil and Pizzo, 1999; Vandas and Odstrčil, 2000) also showed that flux ropes continued to expand when γ is larger than 1.

Flux ropes in space are generally connected to some regions electromagnetically unless they are closed structures such as tori. For example, magnetic field lines of a flux rope emerging from the Sun are often connected to the solar surface, and must close. The field-aligned electric current flowing in the flux rope must also close. Hence, we must consider the whole current system including the electric current flowing outside of the flux ropes.

The total electric current flowing in the flux rope decreases for 3D expansions (Shimazu and Vandas, 2002). Nevertheless, because it forms a closed circuit, the change in current flowing in the flux rope, which is controlled by the expansion, should affect the exterior

current in or around the Sun.

The flux rope expansion generates Alfvén waves because the deformation of the magnetic field lines accompanies the expansion. The change in the field-aligned current also generates Alfvén waves, which carry an electric current. The current accompanied by the Alfvén waves compensates the decrease in current in the 3D expansion.

In previous studies of flux rope expansions (for example, Shimazu and Vandas (2002)), the Alfvén wave radiation and the electric current closure outside of the flux rope were not considered. In this paper, the electric current accompanied by the Alfvén waves is considered. We examine the current matching conditions by combining the theories underlying the self-similar expansion of flux ropes and the Alfvén wave current system.

2 Results

2.1 2D self-similar expansion

Using a cylindrical coordinate system (r, θ, z) that moves with the flux rope, solutions were sought to the MHD equations,

$$\frac{\partial \rho}{\partial t} + \nabla \cdot (\rho \mathbf{v}) = 0, \quad (1)$$

$$\rho \frac{\partial \mathbf{v}}{\partial t} + \rho (\mathbf{v} \cdot \nabla) \mathbf{v} = -\nabla P + \frac{1}{\mu} (\nabla \times \mathbf{B}) \times \mathbf{B}, \quad (2)$$

$$\frac{\partial (P \rho^{-\gamma})}{\partial t} + (\mathbf{v} \cdot \nabla) (P \rho^{-\gamma}) = 0, \quad (3)$$

and

$$\frac{\partial \mathbf{B}}{\partial t} = \nabla \times (\mathbf{v} \times \mathbf{B}), \quad (4)$$

where t is the elapsed time, ρ the mass density, \mathbf{v} the velocity, P the pressure, μ permeability, \mathbf{B} the magnetic field, and γ the polytropic index. The z -axis is taken to lie along the axis of the cylindrical flux rope; the solution is assumed to have no dependence on z (r -dependence only) for 2D expansions.

Following the procedure described in Osherovich et al. (1995), we let f denote the generating function of the self-similar parameter η , and y the evolution function of time. The solutions of Equations (1), (3), and (4) for 2D expansions are then

$$v_r = \eta \dot{y}, \quad (5)$$

$$B_\theta = (-\eta f' / 2)^{1/2} y^{-1}, \quad (6)$$

$$B_z = (2\mu S D)^{1/2} y^{-2}, \quad (7)$$

$$\rho = -D' \eta^{-1} y^{-2}, \quad (8)$$

and

$$P = K D y^{-2\gamma}, \quad (9)$$

where an overdot signifies the derivative with respect to time t , and a prime signifies the derivative with respect to η , which satisfies

$$\eta = ry^{-1}, \quad (10)$$

$$D = \frac{f + \eta f'/2}{2\mu S\chi}, \quad (11)$$

and χ , S , and K are positive constants. The function f satisfies

$$f' \leq 0 \quad (12)$$

$$f + \eta f'/2 \geq 0 \quad (13)$$

and

$$(f + \eta f'/2)' \leq 0. \quad (14)$$

We take $K \rightarrow 0$ (low plasma beta value). Moreover, being most frequently used in the description of a cylindrical flux rope, f is taken to be in the form

$$f = B_1^2 \{J_0^2(\alpha_1 \eta) + J_1^2(\alpha_1 \eta)\}, \quad (15)$$

where J_0 and J_1 are Bessel functions of the first kind of orders 0 and 1, respectively, and B_1 and α_1 are constants. Hence, the magnetic field of the 2D expansion model is given by

$$B_\theta = B_0 J_1(\alpha r y^{-1}) y^{-1}, \quad (16)$$

$$B_z = B_0 J_0(\alpha r y^{-1}) y^{-2}, \quad (17)$$

where

$$y = 1 + t/t_0, \quad (18)$$

and B_0 , t_0 , and α are constants.

2.2 3D self-similar expansion

We include the effects of an axial expansion (z -direction) as well as a radial expansion. An additional self-similar parameter ξ is introduced by

$$\xi = zy^{-1}. \quad (19)$$

We assume that the radial expansion rate is the same as the axial expansion rate. The solutions of Equations (1), (3), and (4), which satisfy

$$\frac{\partial f}{\partial \xi} = 0 \quad (20)$$

in the simplest case are given by

$$v_r = \eta \dot{y}, \quad (21)$$

$$v_z = \xi \dot{y}, \quad (22)$$

$$B_\theta = (-\eta f'/2)^{1/2} y^{-2}, \quad (23)$$

$$B_z = (2\mu SD)^{1/2}y^{-2}, \quad (24)$$

$$\rho = -G'\eta^{-1}y^{-3}, \quad (25)$$

and

$$P = KGy^{-3\gamma}, \quad (26)$$

where G is a function of η and ξ (Shimazu and Vandas, 2002).

With $K \rightarrow 0$ and f as given in Equation (15), the magnetic field of the flux rope for the 3D expansion is expressed as

$$B_\theta = B_0 J_1(\alpha ry^{-1})y^{-2}, \quad (27)$$

$$B_z = B_0 J_0(\alpha ry^{-1})y^{-2}. \quad (28)$$

The expression for B_z is similar to the field solution in the 2D expansion model. The difference in the dependence of B_θ on y (or t) stems from the volume increase in the axial direction. This is the essential effect of the axial expansion. As is easily demonstrated, the total electric current is conserved in the 2D expansion model, whereas the magnetic helicity and the magnetic flux are not conserved. In contrast, the magnetic flux and magnetic helicity in the flux rope is conserved in the 3D expansion model, whereas the total electric current decreases with time (Shimazu and Vandas, 2002).

2.3 Alfvén wave current system

We adopt Alfvén wing theory for the electric current system generated by the Alfvén waves. This theory was developed originally to describe the interaction between a flowing magnetized plasma and a conductor (Drell et al., 1965; Wright and Schwartz, 1990). Consider a conductor moving across a uniform magnetic field \mathbf{B} in a plasma with a velocity \mathbf{v} . The Alfvén waves radiate from the polarization charges and carry an electric current into the surrounding plasma. The magnetic field lines in the plasma act as transmission lines for Alfvén waves. The region through which the Alfvén waves propagate is called the “Alfvén wing”. The theory of the Alfvén wing was advanced largely in studies of the electromagnetic coupling between the Jovian magnetosphere and the Jovian satellite, Io (Neubauer, 1980; Goertz, 1980; Southwood et al., 1980). The Voyager and Galileo satellites detected disturbances of the plasma velocity and magnetic fields associated with the generation of the Alfvén wing around Io (Acuña et al., 1981; Chust et al., 2005).

From the current continuity condition, the induced current J flowing in the conductor and the Alfvén wing is expressed as

$$J = |\mathbf{v} \times \mathbf{B}|a \frac{2\Sigma_I \Sigma_A}{\Sigma_I + 2\Sigma_A}, \quad (29)$$

where a is the length scale of the voltage or current generator, Σ_I the conductance of the conductor, and Σ_A the Alfvén conductance, which is related to the polarization current flowing in the wave front (Hill et al., 1983). If $v/V_A \ll 1$, we have

$$\Sigma_A \equiv \frac{1}{\mu V_A}, \quad (30)$$

where $V_A \equiv B/\sqrt{\mu\rho}$ is the Alfvén velocity (Neubauer, 1980). Note that Σ_A is finite, even though the plasma conductivity is infinitely large. In addition, J remains finite, even as Σ_I tends to infinity; see Equation (29). We consider two extreme cases (Shimazu and Terasawa, 1995): $\Sigma_I \gg \Sigma_A$, called an Alfvénic case with

$$J = 2|\mathbf{v} \times \mathbf{B}|a\Sigma_A, \quad (31)$$

and $\Sigma_I \ll \Sigma_A$ a diffusive case with

$$J = |\mathbf{v} \times \mathbf{B}|a\Sigma_I. \quad (32)$$

2.4 Combining the two theories

In this paper, we include the electric current associated with the flux rope and consider the whole closed current system. We exclude isolated flux ropes that are not connected elsewhere electromagnetically. Consider a flux rope expanding near the solar surface and divide the whole closed current circuit into two regions (Figure 2): the expanding flux rope and the connected region (region excluding the flux rope). The expansion of the flux rope generates Alfvén waves through the deformation of the magnetic field lines and the change in the field-aligned current. The current flowing in the flux rope must close with that carried by the Alfvén waves.

This system is equivalent to an electric circuit (Figure 3) with Σ_I representing the conductance of the connected region, and Σ_A the Alfvén conductance in the flux rope. The expansion of the flux rope corresponds to the source of current or voltage. They constitute a closed circuit.

We apply the Alfvén wing theory to the Alfvén wave current system generated by the flux rope expansion. Of course, an Alfvén wing is not generated in the system we are considering. However, a similar current circuit as in the Alfvén wing system is generated in this system. To apply the Alfvén wing theory, we examine the dependence of J on y by combining the self-similar flux rope expansion model.

In the expanding flux rope, the electric field in the axial direction is generated by the radial expansion. The electric field is given by $|\mathbf{v} \times \mathbf{B}|_z = |v_r B_\theta| \sim y^{-2}$ for the 3D expansion and $\sim y^{-1}$ for the 2D expansion, respectively. As Σ_A has the form $\sim \rho^{1/2} B_\theta^{-1}$, $\Sigma_A \sim y^{1/2}$ for 3D expansions, and $\Sigma_A \sim y^0$ for 2D expansions (no dependence on y). Therefore, in the Alfvénic case, Equation (31) leads to

$$J \sim y^{-1/2}, \quad (33)$$

for 3D expansions, and

$$J \sim y^0, \quad (34)$$

for 2D expansions. Note that $a \sim v_r y$. When Σ_I is assumed constant, Equation (32) in the diffusive case leads to

$$J \sim y^{-1}, \quad (35)$$

for 3D expansions and

$$J \sim y^0, \quad (36)$$

for 2D expansions.

Because J must agree with the current maintaining the magnetic field of the flux rope,

$$J = \frac{2\pi}{\mu} \int_0^a \frac{\partial B_\theta}{\partial r} r dr, \quad (37)$$

the dependence of J on y is given by

$$J \sim y^{-1}, \quad (38)$$

for 3D expansions, and

$$J \sim y^0, \quad (39)$$

for 2D expansions.

We compare Equations (38) and (39) with Equations (33) – (36). For 3D diffusive cases, the dependences on y in Equations (35) and (38) agree; for 2D diffusive cases, Equations (36) and (39) agree. These agreements show that closure is attained between the current flowing in the flux rope and the real current flowing in the connected region. Hence, diffusion (Σ_I) is necessary in the connected region. In this diffusive expansion, both 3D and 2D expansions are possible. However, the 3D diffusive expansion is more applicable because the expansion continues when γ is larger than 1.

In addition, dependences on y in Equations (34) and (39) also agree for the 2D Alfvénic case. In this case, the current flowing in the flux rope closes with that carried by the Alfvén waves. Table 1 shows the possible combinations for these expansions.

3 Discussion

To summarize the previous section, the 3D diffusive expansion and the 2D diffusive expansion are possible when $\Sigma_I \ll \Sigma_A$. A possible alternative case is the 2D Alfvénic expansion when $\Sigma_I \gg \Sigma_A$.

Two-step solar filament eruptions may be interpreted as a transition from one expansion to another. Sometimes the filament eruption decelerates and stops at some height in the corona. After several hours the filament rises again and forms a CME (Byrne et al., 2014; Gosain et al., 2016; Chanda et al., 2017). One of the attractive models of filament eruptions is the catastrophes in the system equilibrium. Van Tend and Kuperus (1978) showed that the equilibrium of a linear electric current in the coronal magnetic field is unstable depending on spatial properties of the coronal field. Priest and Forbes (1990) analyzed in detail the equilibrium and dynamics of a straight flux tube in a background magnetic field of a horizontal dipole located below the conductive surface (photosphere). They showed that a loss of equilibrium in the system causes an eruption of the filament (Schmieder et al., 2015; Filippov, 2018).

Here, we apply our flux rope expansion model to the two-step filament eruptions. When the flux rope starts to expand, Alfvén waves are generated carrying an electric current. The expansion is Alfvénic because the Lundquist number $\Sigma_I/\Sigma_A = \mu V_A \Sigma_I$ is much larger than 1. Even in weakly ionized regions such as the photosphere and the chromosphere, the Lundquist number is larger than 10^4 . In Alfvénic expansions, only the

2D expansion is possible, and because it does not involve an axial expansion, the ascension of the flux rope is relatively small. Moreover, the 2D expansion does not continue when γ is larger than 1, and hence the expansion stops at some level.

After the launch of a CME, the flux rope propagates in interplanetary space. As $\Sigma_I/\Sigma_A \ll 1$, diffusive expansion occurs. Note that Σ_I is for the connected region in or very close to the Sun and Σ_A is for the flux rope in interplanetary space. Because an axial expansion accompanies a 3D expansion, the flux rope ascends rapidly. To trigger the transition from a 2D Alfvénic expansion to a 3D diffusive expansion, there should be some processes to reduce Σ_I in the connected region. For example, reconnection in the connected region and a change in the current circuit may trigger a transition.

If this process works, the initial 2D Alfvénic expansion is a source of Alfvén waves in the solar atmosphere. There is much research showing that Alfvén waves are responsible for heating of the solar atmosphere (Osterbrock, 1961; Ionson, 1978; Hollweg, 1991; Sakurai et al., 1991). Alfvén or transverse mode MHD waves have been observed in the solar photosphere, chromosphere, and corona in some detail using instruments onboard satellite missions and ground-based solar telescopes (Aschwanden et al., 1999; Nakariakov et al., 1999; Ofman and Wang 2008; McIntosh et al., 2011; Okamoto et al., 2015; Antolin et al., 2015).

4 Summary

We included the electric current associated with the expanding magnetic flux rope and considered the whole closed current system. By combining the theories of the self-similar expansion of cylindrical flux ropes and the Alfvén wave current system, we examined those conditions for which the time dependence of the current flowing in the closed circuit agrees with that of the current sustaining the expanding flux rope.

The results have shown that there are three possible expansions: 3D diffusive, 2D diffusive, and 2D Alfvénic expansions. The 3D and 2D diffusive expansions occur when $\Sigma_I/\Sigma_A \ll 1$. In this case, diffusion in the connected region is necessary for the flux rope expansion. The remaining case is the 2D Alfvénic expansion occurring when $\Sigma_I/\Sigma_A \gg 1$. The current flowing in the flux rope then closes with the current carried by the Alfvén waves.

The two-step solar filament eruptions may be interpreted as a transition from the 2D Alfvénic expansion to the 3D diffusive expansion. When the flux rope starts to expand, Alfvén waves are generated and carry the electric current. The 2D Alfvénic expansion occurs, because $\Sigma_I/\Sigma_A \gg 1$. Because the 2D expansion does not involve an axial expansion, the ascension of the flux rope is relatively small. In addition, the expansion does not continue, because γ is larger than 1 and thus, stops at some level.

After the launch of a CME, the flux rope propagates in interplanetary space. Because $\Sigma_I/\Sigma_A \ll 1$, a 3D diffusive expansion should occur. Note that Σ_I is for the connected region in or very close to the Sun and Σ_A is for the flux rope in interplanetary space. Because an axial expansion accompanies the 3D expansion, the flux rope ascends rapidly. To trigger the transition from a 2D Alfvénic expansion to a 3D diffusive expansion, there should be some processes to increase the diffusion in the connected region.

Our interpretation of the two-step filament eruptions did not include considering the stability of the flux rope in the background plasma and magnetic field. We also did not include the curvature of the flux rope axis, the details of the electric current closure or the Alfvén wave propagation outside of the flux rope. We had restricted our attention solely to self-similar expansions. However, this study is our first step with the new interpretation. We intend next to study its consistency with respect to the theory of the loss of equilibrium.

Acknowledgments

The author thanks Yasuhiro Murayama (National Institute of Information and Communications Technology, Japan) for his stimulating and insightful comments and suggestions during the course of this work. This work was supported by NICT 320163 and 190102.

References

- Acuña, M.H., Neubauer, F.M., Ness, N.F.: 1981, *J. Geophys. Res.* **86**, 8513.
- Antolin, P., Okamoto, T.J., De Pontieu, B., Uitenbroek, H., Van Doorselaere, T., Yokoyama, T.: 2015, *Astrophys. J.* **809**, 72.
- Aschwanden, M.J., Fletcher, L., Schrijver, C.J., Alexander, D.: 1999, *Astrophys. J.* **520**, 880.
- Aulanier G., Török T., Démoulin P., DeLuca E.E.: 2010, *Astrophys. J.* **708**, 314.
- Berdichevsky, D.B., Lepping, R.P., Farrugia, C. J.: 2003, *Phys. Rev. E* **67**, 036405.
- Bernstein, I.B., Kulsrud, R.M.: 1965, *Astrophys. J.* **142**, 479.
- Burlaga, L., Sittler, E., Mariani, F., Schwenn, R.: 1981, *J. Geophys. Res.* **86**, 6673.
- Byrne J.P., Morgan H., Seaton D.B., Bain H.M., Habbal S.R.: 2014, *Solar Phys.* **289**, 4545.
- Chandra, R., Filippov, B., Joshi, R., Schmieder, B.: 2017, *Solar Phys.* **292**, 81.
- Chen, J.: 1996, *J. Geophys. Res.* **101**, 27499.
- Chen, J., Garren, D.A.: 1993, *Geophys. Res. Lett.* **20**, 2319.
- Cheng, X., Ding, M.D., Guo, Y., Zhang, J., Vourlidas, A., Liu, Y.D., Olmedo, O., Sun, J.Q., Li, C.: 2014, *Astrophys. J.* **780**, 28.
- Chust, T., Roux, A., Kurth, W.S., Gurnett, D.A., Kivelson, M.G., Khurana, K.K.: 2005, *Planet. Space Sci.* **53**, 395.
- Dasso, S., Nakwacki, M.S., Démoulin, P., Mandrini, C.H.: 2007, *Solar Phys.* **244**, 115.
- DeVore, C.R., Antiochos, S.K.: 2000, *Astrophys. J.* **539**, 954.
- Drell, S.D., Foley, H.M., Ruderman, M.A.: 1965, *J. Geophys. Res.* **70**, 3131.
- Filippov, B.: 2018, *Mon. Not. Roy. Astron. Soc.* **475**, 1646.
- Gary, G.A., Moore, R.L.: 2004, *Astrophys. J.* **611**, 545.
- Gibson, S.E., Low, B.C.: 1998, *Astrophys. J.* **493**, 460.
- Goertz, C.K.: 1980, *J. Geophys. Res.* **85**, 2949.
- Gosain, S., Filippov, B., Ajour Maurya, R., Chandra, R.: 2016, *Astrophys. J.* **821**, 85.
- Hill, T.W., Dessler, A.J., Goertz, C.K.: 1983, Magnetospheric models, in *Physics of the Jovian Magnetosphere*, edited by A.J. Dessler, pp. 365-372, Cambridge Univ. Press, New York.
- Hollweg, J.V.: 1991, in *Mechanisms of Chromospheric and Coronal Heating*, edited by P. Ulmschneider, E.R. Priest, R. Rosner, p. 423, Springer, Berlin.
- Ionson, J.A.: 1978, *Astrophys. J.* **226**, 650.
- Joshi, N.C., Srivastava, A.K., Filippov, B., Kayshap, P., Uddin, W., Chandra, R., Prasad Choudhary, D., Dwivedi, B.N.: 2014, *Astrophys. J.* **787**, 11.
- Kulsrud, R.M., Bernstein, I.B., Kruskal, M., Fanucci, J., Ness, N.: 1965, *Astrophys. J.* **142**, 491.
- Kumar, A., Rust, D.M.: 1996, *J. Geophys. Res.* **101**, 15667.
- Lepping, R.P., Jones, J.A., Burlaga, L.F.: 1990, *J. Geophys. Res.* **95**, 11957.
- Low, B.C.: 1982, *Astrophys. J.* **254**, 796.
- Marubashi, K.: 1986, *Adv. Space Res.* **6(6)**, 335.
- McIntosh, S.W., de Pontieu, B., Carlsson, M., Hansteen, V., Boerner, P., Goossens, M.: 2011, *Nature* **475**, 477.
- Nakariakov, V.M., Ofman, L., Deluca, E.E., Roberts, B., Davila, J.M.: 1999, *Science* **285**,

862.

- Neubauer, F.M.: 1980, *J. Geophys. Res.* **85**, 1171.
- Odstrčil, D., Pizzo, V.J.: 1999, *J. Geophys. Res.* **104**, 483.
- Ofman, L., Wang, T.J.: 2008, *Astrophys. J.* **482**, L9.
- Okamoto, T.J., Antolin, P., De Pontieu, B., Uitenbroek, H., Van Doorselaere, T., Yokoyama, T.: 2015, *Astrophys. J.* **809**, 71.
- Osherovich, V.A., Farrugia, C.J., Burlaga, L.F.: 1993, *J. Geophys. Res.* **98**, 13225.
- Osherovich, V.A., Farrugia, C.J., Burlaga, L.F.: 1995, *J. Geophys. Res.* **100**, 12307.
- Osterbrock, D.E.: 1961, *Astrophys. J.* **134**, 347.
- Panasenco O., Martin S.F., Velli M.: 2014, *Solar Phys.* **289**, 603.
- Patsourakos S., Vourlidas A., Stenborg G.: 2013, *Astrophys. J.* **764**, 125.
- Priest E.R., Forbes T.G.: 1990, *Solar Phys.* **126**, 319.
- Sakurai, T., Goossens, M., Hollweg, J.V.: 1991, *Solar Phys.* **133**, 227.
- Schmieder, B., Aulanier, G., Vršnak, B.: 2015, *Solar Phys.* **290**, 3457.
- Shimazu, H., Terasawa, T.: 1995, *J. Geophys. Res.* **100**, 16923.
- Shimazu, H., Vandas, M.: 2002, *Earth Planets Space* **54**, 783.
- Southwood, D.J., Kivelson, M.G., Walker, R.J., Slavin, J.A.: 1980, *J. Geophys. Res.* **85**, 5959.
- Vandas, M., Fischer, S., Dryer, M., Smith, Z., Detman, T.: 1995, *J. Geophys. Res.* **100**, 12285.
- Vandas, M., Odstrčil, D.: 2000, *J. Geophys. Res.* **105**, 12605.
- Van Tend, W., Kuperus, M.: 1978, *Solar Phys.* **59**, 115.
- Wright, A.N., Schwartz, S.J.: 1990, *J. Geophys. Res.* **95**, 4027.
- Wu, S.T., Guo, W.P., Dryer, M.: 1997, *Solar Phys.* **170**, 265.

Table 1: Possible combinations of the expansion and the dependence of J on y .

diffusive ($\Sigma_I/\Sigma_A \ll 1$)		Alfvénic ($\Sigma_I/\Sigma_A \gg 1$)	
3D	2D	3D	2D
y^{-1}	y^0	-	y^0

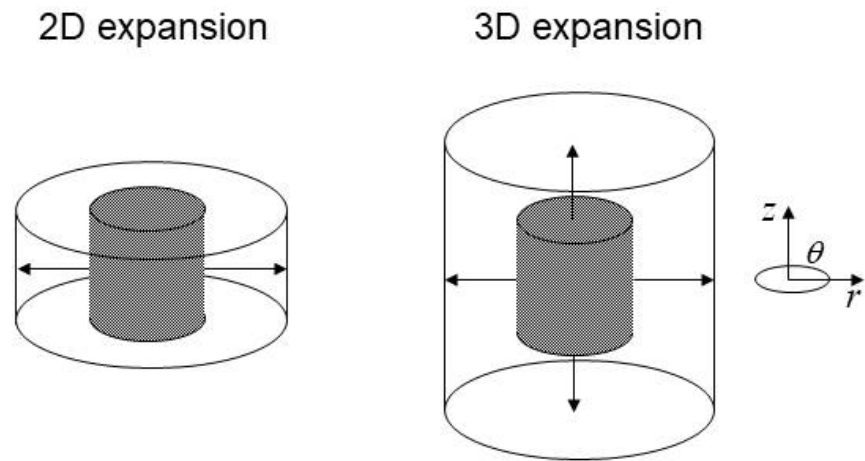


Figure 1.
Schematic illustration of the 2D and 3D expansion models of cylindrical flux ropes.

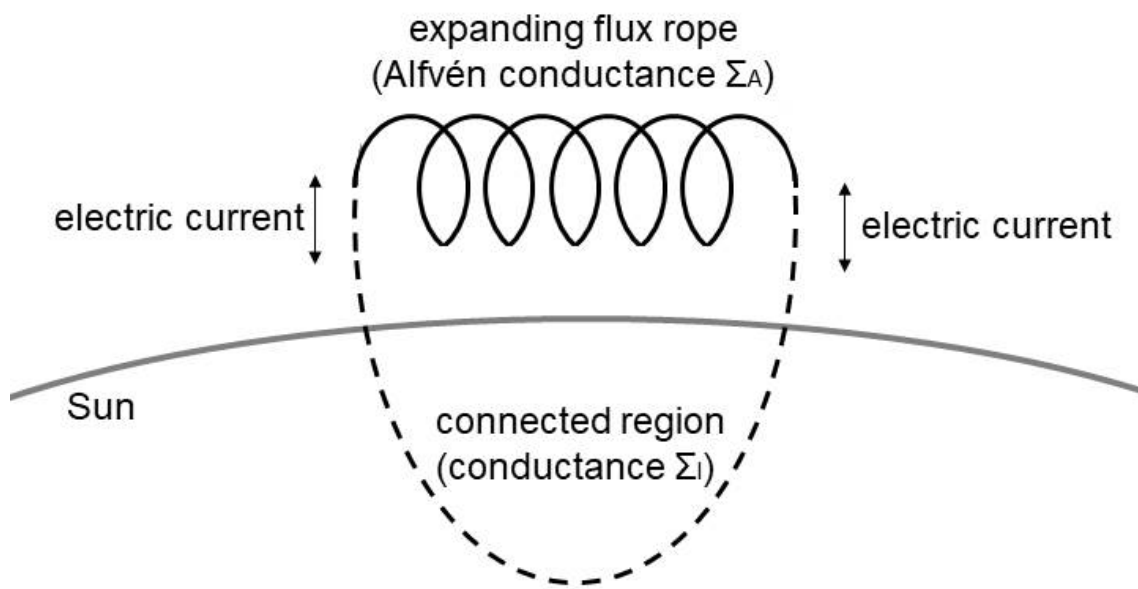


Figure 2.
Schematic illustration of the flux rope expansion model near the solar surface.

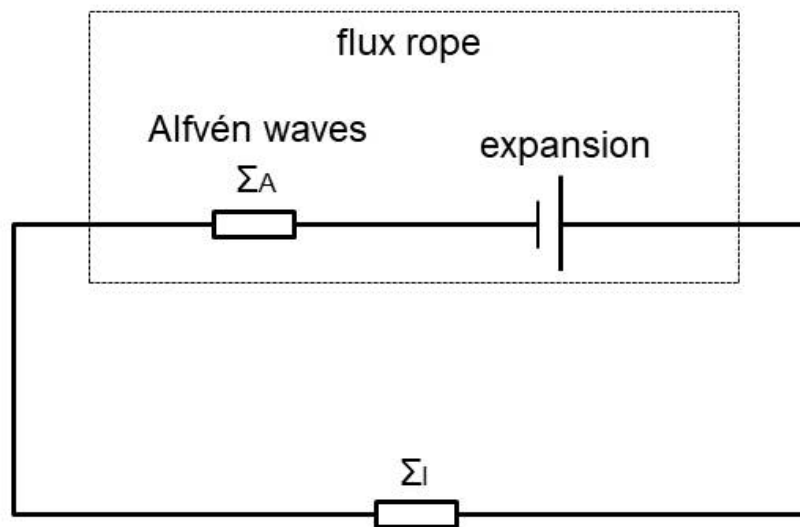


Figure 3.
Equivalent electric circuit for the flux rope expansion. Σ_I is the conductance of the connected region and Σ_A is the Alfvén conductance.